Measurement of the Isotopic Composition of the Iron-Group Elements in the Galactic Cosmic Radiation

G. Tarlé, S. P. Ahlen, and B. G. Cartwright[(a)]
Department of Physics, University of California, Berkeley, California 94720

(Received 30 May 1978)

With an average $\sigma \approx 0.65$ amu we have measured the isotopic composition of Cr, Mn, Fe, and Ni in the galactic cosmic radiation for energies ~ 300 to ~ 600 MeV/amu at the detector. Large deviations from solar-system source composition reported by other workers are not observed.

Measurements of the isotopic composition of the cosmic radiation provide us with the most definitive information concerning their nucleosynthetic origin and the conditions of galactic propagation. In particular, the iron-group isotopes represent the most unbiased cosmic-ray sample in that corrections for nuclear spallation are small, and rigidity-dependent selection effects have a negligible effect on isotopic ratios for a given element.[1] Unfortunately, the small fractional mass difference (~ 2%) between adjacent isotopes of iron has made it difficult to obtain meaningful information in this region. Previous claims of iron-group isotope resolution[2-6] have not been generally accepted as convincing.[7]

The IRIS iron isotope experiment described herein employs a novel combination of both passive and active detectors to measure the mass of iron-group nuclei at energies $E \sim 300$ to ~ 600 MeV/amu. We have capitalized on the benefits of both the high velocity sensitivity of Cherenkov detectors,[2] and the Cherenkov-vs-range technique of isotope analysis pioneered by Fisher *et al.*[4] A cross section of the IRIS telescope appears in Fig. 1. A stack consisting of 330 127-μm sheets of Lexan polycarbonate plastic track detector, labeled R, is used to measure particle range, while a large-area Cherenkov detector, labeled CK, provides a precise measure of speed for a given atomic charge. Measurements of energy loss are provided by plastic scintillators S1 and S2, which, in conjunction with Cherenkov measurements, yield charge information. A passive aluminum absorber PA provides a nonhydrogenous material in which a large part of the slowing takes place. Particles which stop in the range stack R and thus do not trigger the anticoincidence scintillator A are identified with events in the active detectors using trajectory information provided by optical spark chambers SC1 and SC2. The anticoincidence detector plays a major role in eliminating from analysis events which undergo charge-changing nuclear interactions, creating light, highly penetrating fragments. A precise zenith angle, used in correcting the detector response, is obtained by using the long lever arm between the spark chambers and the range stack. For a given atomic charge, speed, and zenith angle, the mass can be determined from the measurement of range using the range-energy formulas.

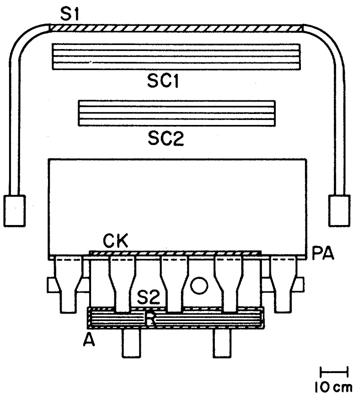

FIG. 1. Schematic outline of the IRIS telescope.

The experiment was flown at ~ 3g/cm^2 residual atmosphere for 25 h from Watertown, South Dakota, on a 2.6×10^7-ft^3 balloon. The cutoff rigidity was less than 1.5 GV during the entire flight for all zenith angles, well below 1.75 GV which corresponds to the threshold energy of the Cherenkov radiator for ^{56}Fe nuclei. During this time 1622 events triggered the coincidence logic $S1 \cdot S2 \cdot \bar{A}$. Of these, 1505 produced acceptable tracks in the spark chambers. To date ~ 600 events have been identified with particle tracks found in the Lexan. The analysis so far has been limited to events of high atomic charge ($Z \geqslant 24$) using a threshold criterion imposed by the track etching rate in the plastic detectors. A detailed discussion of the analysis will be presented elsewhere.

The resolution of the IRIS instrument is limited solely by the photoelectron statistics of the

Cherenkov detector because of the high intrinsic accuracy of the range measurement. In a mock-up of the IRIS instrument, 600-MeV/amu ^{56}Fe ions from the Lawrence Berkeley Laboratory Bevalac stopped ~3% short of that predicted by the Bethe formula[8] and showed a range straggling of $\sigma \lesssim 0.2\%$. This small straggling results from the huge number of collisions with atomic electrons necessary to bring a heavy ion to rest. Before etching, the thickness of all Lexan sheets used in the flight was mapped on a 5-cm grid to an accuracy of ~2 μm to eliminate possible systematic effects on the range measurement.

Preflight calibrations with ^{20}Ne ions from 0 to 550 MeV/amu showed that the Cherenkov signal consisted of three components[9]: (1) primary Cherenkov emission characterized by an index of refraction $n = 1.518 \pm 0.005$; (2) Cherenkov emission by secondary electrons; (3) residual scintillation at $S = 2.7\%$ of the Cherenkov signal for $\beta = 1$. A fit to the iron data from the flight yielded essentially the same values ($n = 1.513$, $S = 2.66\%$) provided the residual scintillation was unsaturated. A recent Bevalac exposure with ^{56}Fe has confirmed this result. From these measurements, we have determined that the photoelectron limited resolution ranges from ~(1–4)% of the Cherenkov signal for iron nuclei over the accepted energy window. Thickness variations in the Cherenkov radiator were mechanically measured and taken into account. Variations in the Cherenkov signal resulting from spatial variation of light-collection efficiency and radiator edge absorption were inferred from measurements using an ^{241}Am-doped NaI-crystal light source. The variations were less than 4% in the central 65% of the area but were so large near the edges that it was necessary to eliminate from analysis all events which traversed CK within ~5 cm of its perimeter. Angular dependence of light-collection efficiency was eliminated by uniformly roughening the surface of the Cherenkov radiator. A temporal drift correction was extracted from the iron data from the flight, using a two-tailed exponential filter with a time constant of 4000 sec. We found that this correction was insensitive to the method of extraction and choice of time constant, had an rms value of 1.5%, and was well correlated with the observed temperature variations during the flight.

Preflight Bevalac calibrations of organic scintillators with ^{20}Ne ions[10] led us to believe that their light output consisted of two components: (1) a "core" term which was saturated as a result of the formation of quenching centers which nonradiatively de-excite activated fluor molecules and (2) an unsaturated "halo" term. A model based on these two components predicted that for high values of specific energy loss dE/dx (such as encountered from Fe nuclei) the light output from the core would be negligible, resulting in a signal which increases linearly with deposited energy with a proportionality constant $\sim\frac{1}{3}$ that obtained with singly charge particles. The iron data from the flight enabled us to improve upon this simplified model. Although the qualitative features of the model were preserved, a small additional light source had to be invoked. After correction for thickness variations (measured with a laser interferometer), light-collection nonuniformity (calculated using a computer code designed for this purpose), and temporal drift, the response of S2 was fitted with the function

$$\frac{dL}{dx} = K\left\{\frac{(1-F_s)dE/dx}{1+B(1-F_s)dE/dx} + F_s\frac{dE}{dx}\right\},$$

where $F_s(T_0, \beta)$ is the fraction of secondary electrons produced with an energy $T_0 > 1500$ eV by an ion at velocity β. Here dL/dx is the specific luminescence, K is a normalization constant, and B is a free parameter determined to be 1.48×10^{-3} (g/cm^2)/MeV. Since the scintillation process is not well understood, we emphasize that S2 is not used in the mass determination.

The charge distributions obtained using CK-R and CK-S2 combinations are shown in Fig. 2. A continuous atomic mass function was used for these charge determinations. This causes an additional spreading at the base of the CK-R charge peaks because of sensitivity to the presence of additional isotopes. Ideally we would like to assign

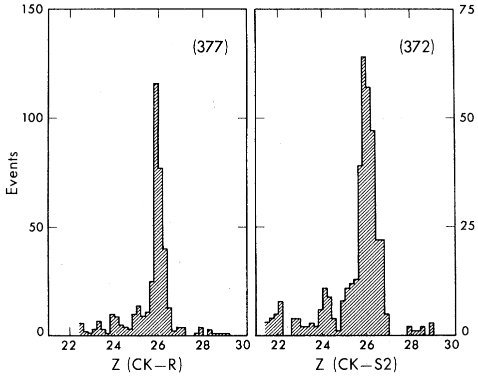

FIG. 2. Charge histograms obtained using CK-R and CK-S2 modes of analysis.

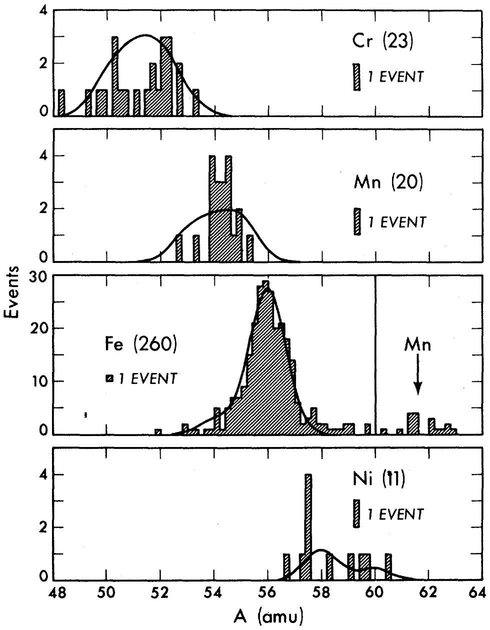

FIG. 3. Mass histograms for Cr, Mn, Fe, and Ni. The solid lines represent abundances calculated assuming a solar system source composition (see text).

an integral charge Z to each event on the basis of CK-S2 and then determine the mass A with CK-R. This is possible for all charges except Mn and Fe, which are not separated in CK-S2. It was thus necessary to separate these two elements using range information. The excellent separation of Ni from Fe is a result of the absence of Co.

Mass histograms for the elements Cr, Mn, Fe, and Ni appear in Fig. 3. The events in the Mn and Fe group were initially treated as $Z=26$. The Mn events were then chosen by arbitrarily placing a cut on the Fe mass distribution at $A=60$ as shown. Events to the right of this line were then treated at $Z=25$ and masses for these events were determined and plotted for Mn. We note that this process makes it impossible to determine the isotopes of Mn with $A \lesssim 53$. The mass resolution obtained as determined from the width of the iron peak is $\sigma \sim 0.65$ amu. This is consistent with our expected resolution of 0.58 amu averaged over all energies. The small number of events precluded our restricting the energy interval to the region just above the Cherenkov threshold where the peak resolution is $\sigma \sim 0.35$ amu. The resolution attained allows us to draw significant new astrophysical conclusions from this cosmic-ray iron-isotope data.

A summary of our measurements appears in Table I. These are compared with abundances that one would obtained from a solar-system-like source composition. For this purpose calculations of galactic propagation have been performed using a 5-g/cm^2 mean exponential pathlength. These results were then corrected with slab-model calculations to account for spallation in the residual atmosphere and telescope. Partial cross sections used were those of Silberberg and Tsao[11,12] scaled using target factors obtained from recent Fe fragmentation experiments.[13,14] Total fragmentation cross sections were those of Karol,[15] adjusted slightly to fit available experimental data.[16] The propagation results normalized at iron have been plotted in Fig. 3 using Gaussian distribution functions at each isotope with $\sigma = 0.65$ amu. As can readily be seen, all our data are consistent, within errors, with a solar-system-like source composition. The large excesses of ^{56}Fe and/or ^{54}Fe reported by other workers[2-6] are not observed. This coupled with the observed absence of a single dominant nickel isotope cannot be reconciled with a single e-process zone[17] as the source of these high-en-

TABLE I. Summary of measurements.

	This work	Solar system + spallation to top of CK (assuming no decay)
^{60}Ni/^{58}Ni	$\sim 0.57 \pm 0.36$	0.38
^{54}Fe/(^{55}Fe + ^{56}Fe + ^{57}Fe)	< 0.10	0.083
^{58}Fe/(^{55}Fe + ^{56}Fe + ^{57}Fe)	< 0.10	0.003
Mn($A > 53$)	54.23 ± 0.15 (mean mass)	^{53}Mn^a:^{54}Mn^b:^{55}Mn $\sim 0.8:1.0:1.2$
Cr	Some ^{50}Cr and ^{52}Cr "dip" at ^{51}Cr	^{50}Cr:^{51}Cr^c:^{53}Cr $\approx 0.6:1.0:1.0:0.3$

[a] e-capture isotope, $\tau_{\rm lab} = 3.6 \pm 0.4 \times 10^6$ yr, β^+ allowed, $\tau = 6 \times 10^4 - 1 \times 10^7$ yr.
[b] e-capture isotope, $\tau_{\rm lab} = 314$ days, $\beta^\pm$ allowed, $\tau \sim 2 \times 10^6$ yr.
[c] e-capture isotope, $\tau_{\rm lab} = 28$ days, $\beta^\pm$ not allowed.

ergy cosmic rays. We conclude that either the galactic cosmic rays that form the iron group are swept-up solar-system–like material or are produced in a combination of zones which are indistinguishable, at the present level of accuracy, from these which produced the material which formed the solar system ~ 5×10^9 years ago.

We wish to thank P. B. Price, Jan deVries, M. Solarz, E. K. Shirk, P. Byren, and M. Salamon for valuable contributions. This work was supported by National Aeronautics and Space Administration Grant No. NGR 05-003-376.

(a) Present address: Harvard Law School, Harvard University, Cambridge, Mass. 02139.

[1] S. E. Woosley, Astrophys. Space Sci. **39**, 103 (1976).

[2] W. R. Webber, J. A. Lezniak, and J. Kish, Astrophys. J. Lett. **183**, L81 (1973).

[3] G. A. Simpson, J. Kish, J. A. Lezniak, and W. R. Webber, Astrophys. Lett. **19**, 3 (1977).

[4] A. J. Fisher, F. A. Hagen, F. Maehl, J. F. Ormes, and J. F. Arens, Astrophys. J. **205**, 938 (1976).

[5] W. Enge, Nucl. Instrum. Methods **147**, 211 (1977).

[6] R. P. Henke and E. V. Benton, Nucl. Instrum. Methods **142**, 521 (1977).

[7] C. J. Waddington, in *Proceedings of the International Conference on Cosmic Rays, Plovdiv, Bulgaria, 1977* (Bulgarian Academy of Sciences, Plovdiv, Bulgaria, 1977).

[8] G. Tarlé and M. Solarz, Phys. Rev. Lett. **41**, 483 (1978).

[9] S. P. Ahlen, B. G. Cartwright, and G. Tarlé, Nucl. Instrum. Methods **136**, 235 (1976).

[10] S. P. Ahlen, B. G. Cartwright, and G. Tarlé, Nucl. Instrum. Methods **147**, 321 (1977).

[11] R. Silberberg and C. H. Tsao, Astrophys. J. Suppl. **25**, 315 (1973).

[12] R. Silberberg and C. H. Tsao, in *Proceedings of the Fifteenth International Conference on Cosmic Rays, Plovidv, Bulgaria, 1977* (Bulgarian Academy of Science, Plovdiv, Bulgaria, 1977), Vol. 2, p. 84.

[13] G. D. Westfall, P. J. Lindstrom, D. E. Greiner, H. J. Crawford, L. W. Wilson, and H. H. Heckman, Bull. Am. Phys. Soc. **23**, 27 (1978), Abstract BE4.

[14] G. D. Westfall, private communication.

[15] P. J. Karol, Phys. Rev. C **11**, 1203 (1975).

[16] P. J. Lindstrom, D. E. Greiner, H. H. Heckman, B. Cork, and F. S. Bieser, in *Proceedings of the Fourteenth International Conference on Cosmic Rays, Munich, West Germany, 1975* (Max-Planck-Institut für Extraterrestrische Physik, Garching, West Germany, 1975), Vol. 7, p. 2315.

[17] K. L. Hainenbach, D. D. Clayton, W. D. Arnett, and S. E. Woosley, Astrophys. J. **193**, 157 (1974).